Molecular Mechanics Analysis of Structure and Diastereoselectivity toward Lithiation in Amido- and α-Aminoferrocene Complexes

James A. S. Howell,* Paul C. Yates, and Natalie Fey†

Lennard-Jones Laboratories, School of Chemistry and Physics, Keele University, Staffordshire ST5 5BG, United Kingdom

Patrick McArdle and Desmond Cunningham

University College, Galway, Ireland

Simon Parsons and David W. H. Rankin

Department of Chemistry, University of Edinburgh, West Mains Road, Edinburgh EH9 3JJ, United Kingdom

Received July 12, 2002

A molecular mechanics force field has been developed for the conformational analysis of amido- and α-aminoferrocenes. Parameterization for ring-substituent rotational barriers in amidoferrocenes and other cross-conjugated derivatives have been calculated using DFT on both the free and complexed cyclopentadienyl ligand. Modeled structures of (diisopropylamido)- and (dimethylamido)ferrocene and *N*,*N*-dimethyl-α-ferrocenylethylamine are in agreement with those determined through single-crystal X-ray diffraction. The diastereoselective lithiation of *N*,*N*-dimethylferrocenylethylamine and sparteine-mediated enantioselective lithiation of (diisopropylamido)ferrocene using MeLi have been modeled through an assumed reversible adduct formation at the amine nitrogen or amide oxygen, followed by an irreversible ring lithiation. Results indicate that selectivity results from ring lithiation via the adduct conformer with the shortest $C-H_{ring}$- - -H_3C-Li interaction.

Introduction

The design and synthesis of chiral ferrocenyl ligands for use in asymmetric catalysis continue to attract widespread interest.[1] Many effective ligands combine both central chirality in the form of an α- or *β*-stereogenic center with planar chirality in the form of ortho ring substitution on one or both cyclopentadienyl rings. Though enantiopure compounds with planar-only chirality may be obtained by classical resolution,[2] chromatography,[3] or enzymatic methods,[4] substantial recent progress has been concerned mainly with asymmetric methods for the introduction of planar chirality. Historically, such work dates to the discovery of the highly diastereoselective ortho-lithiation of *N*,*N*-dimethyl-α-ferrocenylethylamine (**1**) by Ugi and co-workers (Scheme 1).[5]

Scheme 1[a]

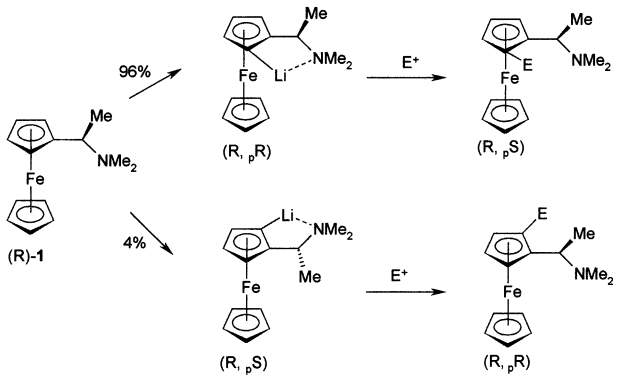

[a] The planar chirality assignments are based on electrophiles with CIP priority higher than that of the alkylamino substituent.

The easy availability of **1** as both enantiomers,[6,7] the range of quenching electrophiles which may be used, and the ease of stereospecific nucleophilic displacement at the α-stereogenic carbon continue to make this

* To whom correspondence should be addressed. Fax: +44 1782 712378. E-mail: jashowell@chem.keele.ac.uk.

† Current address: Department of Chemistry, University of Warwick, Coventry CV4 7AL, U.K.

(1) (a) *Metallocenes. Synthesis, Reactivity, Applications*; Togni, A., Halterman, R. L., Eds. Wiley-VCH: Weinheim, Germany, 1998. (b) Richards, C. J.; Locke, A. J. *Tetrahedron*: *Asymmetry* **1998**, *9*, 2377. (c) Riant, O.; Kagan, H. B. In *Advances in Asymmetric Synthesis*; Hassner, A., Ed.; JAI Press: London, 1997; Vol. 2, p 189.

(2) See, for example: Westman, L.; Rinehart, K. L. *Acta Chem. Scand.* **1962**, *16*, 1189.

(3) See, for example: (a) Wally, H.; Nettekoven, U.; Weissensteiner, W.; Werner, A.; Widhalm, M. *Enantiomer* **1997**, *2*, 441. (b) Reety, M. T.; Beuttenmüller, E. W.; Goddard, R.; Pastó, M. *Tetrahedron Lett.* **1999**, *40*, 4977.

(4) See, for example: (a) Patti, A.; Lambusta, D.; Piatelli, M.; Nicolosi, G. *Tetrahedron*: *Asymmetry* **1998**, *9*, 3073. (b) Malfait, S.; Pelinksi, L.; Brocard, J. *Tetrahedron*: *Asymmetry* **1998**, *9*, 2207, 2595. (c) Delacroix, O.; Picart-Goetgheluck, S.; Maciejewski, L.; Brocard, J. *Tetrahedron*: *Asymmetry* **1999**, *10*, 1835, 4417.

(5) Marquarding, D.; Klusacek, H.; Gokel, G. W.; Hoffmann, P.; Ugi, I. K. *J. Am. Chem. Soc.* **1970**, *92*, 5389.

(6) Gokel, G. W.; Ugi, I. K. *J. Chem. Educ.* **1972**, *49*, 294.

(7) For enzymatic resolutions of **1**, see: (a) Iglesias, L. E.; Rebolledo, F.; Gotor, V. *Tetrahedron*: *Asymmetry* **2000**, *11*, 1047. (b) Kijima, T.; Yagimum, Y.; Izumi, T. *J. Chem. Technol. Biotechnol.* **1999**, *74*, 501.

10.1021/om020556q CCC: $22.00
Publication on Web 10/23/2002

compound a widely used precursor.[8] Enantiomeric excesses of >97% have been achieved by replacing the α-methyl group with ethyl, pentyl, phenyl, *o*-tolyl, *o*-bromophenyl, and 2-naphthyl substituents. Use of 1,1′-disubstituted α-aminoferrocenes also appears to improve selectivity.[9a] Structurally varied derivatives of **1** may be prepared inter alia by auxiliary-controlled imine reduction,[10] by auxiliary-controlled alkylation of hydrazones,[11] by catalyst-controlled alkylation of aldehydes,[9c] or from a range of enantiopure alcohols of structure **2** prepared either by enzymatic resolution[12] or by asymmetric reduction of ferrocenyl ketones.[9a,b,e,13]

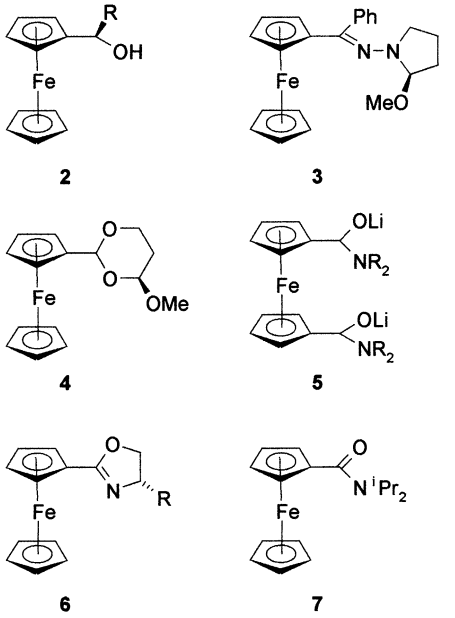

Methyl ethers of **2** also undergo diastereoselective lithiation,[14] as do the hydrazone **3**,[15] the acetal **4**,[16a–c] the aminal **5**,[17] and oxazolines of structure **6**.[18] Achiral carboxamides such as **7** undergo a highly enantioselective sparteine-mediated ortho lithiation.[19]

Rational ferrocenyl ligand design would be facilitated by a reliable molecular mechanics (MM) protocol, which was sensitive to small changes in inter-ring and ring-substituent interactions. We have recently implemented a force-field approach which reproduces accurately the structures of monoalkyl- and 1,1′-dialkylferrocenes.[20] In this article, we wish to report how this may be extended to ferrocenyl complexes with cross-conjugated substituents and how molecular mechanics may be applied in an interpretive and predictive fashion to two of the diastereoselective reactions described above, namely the ortho lithiation of **1** and ether derivatives of **2** and the sparteine-mediated ortho lithiation of **7**.

Results and Discussion

The mechanism or mechanisms of the ortho-lithiation process remain a subject of debate.[21] However, it seems likely that for amine, amide, and other directing groups containing strong donor atoms, the reaction may be viewed as a reversible coordination of the lithium at the donor site, followed by a rate-determining and irreversible transfer of lithium to the ortho position.[21b] We have therefore sought to determine the preferred conformations of the free amino- and amidoferrocenes, the effect of initial lithium complexation on the substituent rotational energy profile, and the influence of substituent effects on the stability of the lithiated intermediates. Some assumptions have been made for calculational simplicity, namely the neglect of charge interactions and

(8) See, for example: (a) Rampf, F. A.; Herrmann, W. A. *J. Organomet. Chem.* **2000**, *601*, 138. (b) Ito, Y.; Kuwano, R. *Phosphorus, Sulfur Silicon Relat. Elem.* **1999**, *144–46*, 469. (c) Burckhardt, U.; Drommi, D.; Togni, A. *Inorg. Chim. Acta* **1999**, *296*, 183. (d) Pioda, G.; Togni, A. *Tetrahedron*: *Asymmetry* **1998**, *9*, 3903. (e) Fukuzawa, S.; Kato, H. *Synlett* **1998**, 727. (f) Takada, H.; Nishibayashi, Y.; Uemura, S.; Asai, T.; Ito, Y.; Redon, M.; Krief, A. *Bull. Chem. Soc. Jpn.* **1997**, *70*, 2807. (h) Song, J. H.; Cho, D. J.; Jeon, S. J.; Kim, Y. H.; Kim, T. J.; Jeong, J. H. *Inorg. Chem.* **1999**, *38*, 893. (i) Shirahata, M.; Yamazaki, H.; Fukuzawa, S. *Chem. Lett.* **1999**, 245. (j) Beyer, L.; Richter, R.; Seidelmann, O. *J. Organomet. Chem.* **1998**, *561*, 199. (k) Lu, X.; Chen, G. *Tetrahedron* **1998**, *54*, 12539.

(9) (a) Almena Perea, J. J.; Borner, A.; Knochel, P. *Tetrahedron Lett.* **1998**, *39*, 8073. (b) Almena Perea, J. J.; Lotz, M.; Knochel, P. *Tetrahedron*: *Asymmetry* **1999**, *10*, 375. (c) Kan, J.; Lee, J. H.; Ahn, S. H.; Choi, J. S. *Tetrahedron Lett.* **1998**, *39*, 5523. (d) Schwink, L.; Knochel, P. *Chem. Eur. J.* **1998**, *4*, 950. (e) Ireland, T.; Grossheimann, G.; Wieser-Jeuness, C.; Knochel, P. *Angew. Chem., Int. Ed. Engl.* **1999**, *38*, 3212. (f) Kang, J.; Lee, J. H.; Kim, J. B. *Chirality* **2000**, *12*, 378.

(10) See, for example: (a) Cayuela, E. M.; Xiao, L.; Sturm, T.; Manzano, B. R.; Jalon, F. A.; Weissensteiner, W. *Tetrahedron: Asymmetry* **2000**, *11*, 861. (b) Bastin, S.; Delebecque, N.; Agbossou, F.; Brocard, J.; Pelinski, L. *Tetrahedron*: *Asymmetry* **1999**, *10*, 1647.

(11) Enders, D.; Lochtman, R. *Eur. J. Org. Chem.* **1998**, 689.

(12) See, for example, ref 7b and: (a) Patti, A.; Nicolosi, G.; Howell, J. A. S.; Humphries, K. *Tetrahedron*: *Asymmetry* **1998**, *9*, 4381. (b) Patti, A.; Nicolosi, G. *Tetrahedron*: *Asymmetry* **2000**, *11*, 815.

(13) See, for example: (a) Schwink, L.; Knochel, P. *Chem. Eur. J.* **1998**, *4*, 950. (b) Richards, C. J.; Locke, A. J. *Organometallics* **1999**, *18*, 3750. (c) Kang, J.; Lee, J. H.; Kim, J. B.; Kim, G. J. *Chirality* **2000**, *12*, 278. (c) Lotz, M.; Ireland, T.; Perea, J. J. A.; Knochel, P. *Tetrahedron*: *Asymmetry* **1999**, *10*, 1839. (d) Schwink, L.; Ireland, T.; Puntener, K.; Knochel, P. *Tetrahedron*: *Asymmetry* **1998**, *9*, 1143.

(14) (a) Lotz, M.; Ireland, T.; Tappe, K.; Knochel, P. *Chirality* **2000**, *12*, 389. (b) Ireland, T.; Perea, J. J. A.; Knochel, P. *Angew. Chem., Int. Ed.* **1999**, *38*, 1457.

(15) (a) Enders, D.; Peter, R.; Lochtman, R.; Runsink, J. *Synlett* **1997**, 1462. (b) Enders, D.; Peters, R.; Runsink, J.; Bats, J. W. *Org. Lett.* **1999**, *1*, 1863. (c) Enders, D.; Peters, R.; Lochtman, R.; Raabe, G. *Angew. Chem., Int. Ed.* **1999**, *38*, 2420.

(16) See, for example: (a) Skibniewski, A.; Bluet, G.; Druze, N.; Riant, O. *Synthesis* **1999**, 459. (b) Neo, A. G.; Gref, A.; Riant, O. *Chem. Commun.* **1998**, 2353. (c) Larsen, A. O.; Taylor, R.; White, P. S.; Gagne, M. *Organometallics* **1999**, *18*, 5157. (d) Iftime, G.; Daran, J. C.; Manoury, E.; Balavoine, *J. Organomet. Chem.* **1998**, *565*, 115.

(17) (a) Balavoine, G. G. A.; Daran, J. C.; Iftime, G.; Manoury, E.; Moreau-Bossuet, C. *J. Organomet. Chem.* **1998**, *567*, 191. (b) Iftime, G.; Dran, J. C.; Manoury, E.; Balavoine, G. G. A. *Angew. Chem., Int. Ed.* **1998**, *37*, 1698.

(18) See, for example: (a) Zang, W.; Yoneda, Y.; Kida, T.; Nakatsuji, Y.; Ikeda, I. *J. Organomet. Chem.* **1999**, *574*, 19. (b) Nishibayashi, Y.; Segawa, K.; Arikawa, Y.; Ohe, K.; Hidai, M.; Uemura, S. *J. Organomet. Chem.* **1997**, *545–546*, 281. (c) Kuwano, R.; Uemura, T.; Saito, M.; Ito, Y. *Tetrahedron Lett.* **1999**, *40*, 1327. (d) Donde, Y.; Overman, L. E. *J. Am. Chem. Soc.* **1999**, *121*, 2933. (e) Pickett, T. E.; Richards, C. J. *Tetrahedron*: *Asymmetry* **1999**, *10*, 4095. (f) Bolm, C.; Muniz-Fernandez, K.; Seger, A.; Raage, G.; Gunter, K. *J. Org. Chem.* **1998**, *63*, 7860. (g) Bolm, C.; Muniz, K. *Chem. Commun.* **1999**, 1295. (h) Bolm, C.; Muniz, K.; Hildebrand, J. P. *Org. Lett.* **1999**, *1*, 491. (i) Deng, W. P.; Hou, X. L.; Dai, L. X.; Dong, X. W. *Chem. Commun.* **2000**, 1483. (j) You, S. L.; Zhou, Y. G.; Hou, X. L.; Dai, L. X. *Chem. Commun.* **1998**, 2765. (k) Deng, W. P.; Hou, X. L.; Dai, L. X.; Yu, Y. H.; Xia, W. *Chem. Commun.* **2000**, 285. (l) You, S. L.; Hou, X. L.; Dai, L. X.; *Tetrahedron*: *Asymmetry* **2000**, *11*, 1495. (m) Manoury, E.; Fossey, J. S.; Ait-Haddou, H.; Daran, J. C.; Balavoine, G. G. A. *Organometallics* **2000**, *19*, 3736.

(19) (a) Tsukazaki, M.; Tinkl, M.; Roglans, A.; Chapell, B. J.; Taylor, N. J.; Snieckus, V. *J. Am. Chem. Soc.* **1996**, *118*, 685. (b) Laufer, L. S.; Veith, U.; Taylor, N. J.; Snieckus, V. *Org. Lett.* **2000**, *2*, 629. (c) Jendralla, H.; Paulus, E. *Synlett* **1997**, 471.

(20) Morrison, C. A.; Bone, S. F.; Rankin, D. W. H.; Robertson, H. E.; Parsons, S.; Coxall, R. A.; Fraser, S.; Howell, J. A. S.; Yates, P. C.; Fey, N. *Organometallics* **2001**, *20*, 2309.

(21) For leading references, see: (a) Chadwick, S. T.; Rennels, R. A.; Rutherford, J. L.; Collum, D. B. *J. Am. Chem. Soc.* **2000**, *122*, 8640. (b) Anderson, D. R.; Faibish, N. C.; Beak, P. *J. Am. Chem. Soc.* **1999**, *121*, 7553. (c) Opitz, A.; Koch, R.; Katritzky, A. R.; Fan, W. Q.; Andres, E. *J. Org. Chem.* **1995**, *60*, 3743. (d) Hommes, N. J. R. v. E.; Schleyer, P. v. R. *Angew. Chem., Int. Ed. Engl.* **1992**, *31*, 755. (e) Hommes, N. J. R. v. E.; Schleyer, P. v. R. *Tetrahedron* **1994**, *50*, 5903.

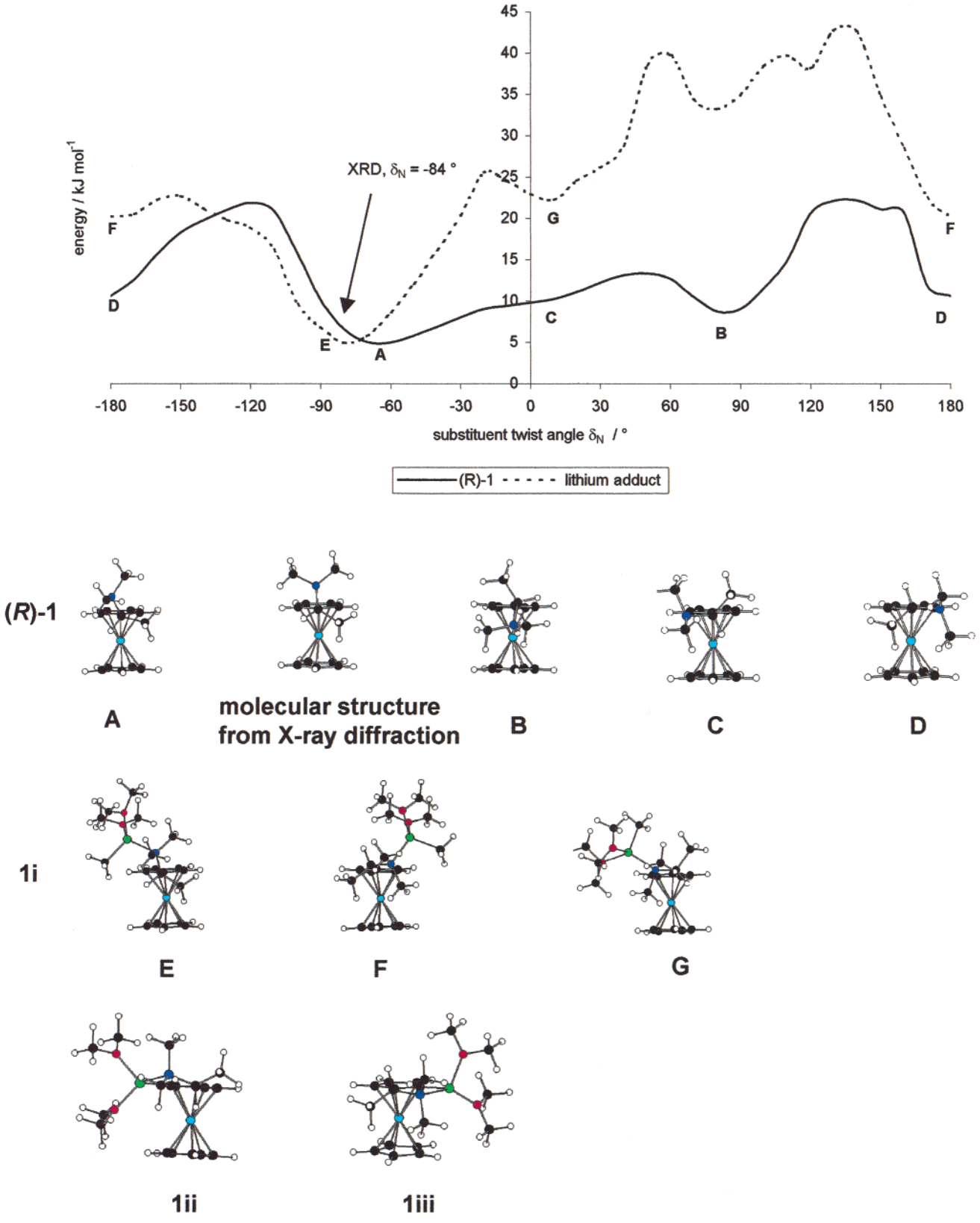

Figure 1. Substituent rotational energy profile for **(*R*)-1** and its MeLi$(Me_2O)_2$ adduct.

solvation effects, nonaggregation of the lithium, and the use of MeLi. Most reported Li−sparteine structures are nonaggregated in the solid state,[22] and recent calculations[23] on the sparteine-meditated lithiation of *N*-Boc-pyrrolidine indicate a dominance of steric effects which should be amenable to analysis by molecular mechanics. Since the alkyllithium reagent may be expected to minimize its ligand profile toward the complex by preferentially adopting conformations with the alkyl chain pointing away from the reacting site, MeLi provides a reasonable model for the ^{n}BuLi used synthetically and eliminates additional conformational degrees of freedom arising from rotation of the alkyl side chain.

Table 1

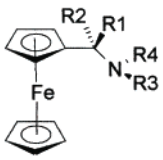

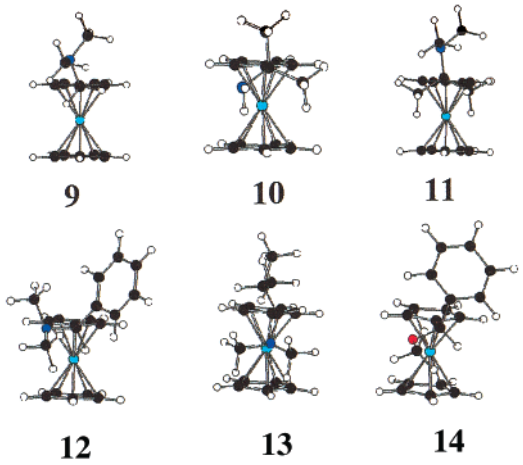

(a) Relative Conformational Energies and Substituent Orientations in Free Alkylamino-and Alkoxyferrocenes

no.	R1	R2	R3	R4	*E*/kJ mol^{-1}	pop. (293 K)/%	$\delta_{N/O}$/deg[a]	no.	R1	R2	R3	R4	*E*/kJ mol^{-1}	pop. (293 K)/%	$\delta_{N/O}$/deg[a]
1	H	Me	Me	Me	0.0	68	−63.8	**11**	Me	Me	Me	Me	0.0	65	−80.4
					3.7	15	81.5						3.6	15	176.2
					4.8	10	−1.0						3.6	15	14.9
					5.6	7	179.1						6.0	6	150.7
8	H	H	H	H	0.00	34	46.1	**12**	H	Ph	Me	Me	0.0	49	−0.2
					0.03	33	135.6						1.9	22	−98.2
					0.06	33	−95.8						2.7	16	167.2
9	H	H	Me	Me	0.0	46	−67.2						3.3	13	142.2
					0.2	42	−122.6	**13**	H	^{i}Pr	Me	Me	0.0	97	80.7
					3.3	12	102.3						8.5	3	−51.2
10	Me	Me	H	H	0.0	41	37.5						16.1	0	−159.0
					0.1	40	144.6	**14**	FcCH(OMe)Ph				0.0	42	21.5
					2.0	18	−87.7						1.5	23	124.7
													2.4	16	−50.2
													3.1	12	−120.9
													4.4	7	1.0

(b) Relative Energies and Selected Geometrical Parameters for **(*R*)-1i**

	E/kJ mol^{-1}	pop. (293 K)/%	δ_N/deg	CH_3−H/Å	Li−C/Å		*E*/kJ mol^{-1}	pop. (293 K)/%	δ_N/deg	CH_3−H/Å	Li−C/Å
E	0.0	100	−79.9	3.03	3.32	G	16.2	0	7.1	3.27	3.30
F	13.8	0	−178.5	3.12	2.71						

(c) Relative Energies and Populations for Lithiated Intermediates

no.	R1	R2	R3	R4	lithiated $_pR,R$ *E*/kJ mol^{-1}	lithiated $_pS,R$ *E*/kJ mol^{-1}	pop. $_pR,R$:$_pS,R$ (293 K)/%	no.	R1	R2	R3	R4	lithiated $_pR,R$ *E*/kJ mol^{-1}	lithiated $_pS,R$ *E*/kJ mol^{-1}	pop. $_pR,R$:$_pS,R$ (293 K)/%
1ii, iii	H	Me	Me	Me	0.00	4.63	87:13	**13ii, iii**	H	^{i}Pr	Me	Me	0.00	8.06	96:4
12ii, iii	H	Ph	Me	Me	0.00	11.72	99:1								

[a] $\delta_{N/O} = C_{ring}-C_{ring}-C_{subst}-N/O$.

A. Ortho Lithiation of 1 and Related Complexes. The conformational space for **(*R*)-1**[24] with respect to ring-substituent rotation was searched using the force field recently developed for alkylferrocenes.[20] The substituent rotational profile shows two local minima with the NMe_2 substituent perpendicular to and in the ring plane (**B** and **D**) and one plateau (**C**) corresponding to the other in-plane orientation. The global minimum (**A**) (Figure 1) shows the NMe_2 group twisted above the plane of the ring ($\delta_N = 64°$). Though **1** is a liquid under ambient conditions, crystals of racemic **1** may be grown by slow cooling in a glass capillary, followed by recording of diffraction data at −123 °C. The molecular structure of **1** in the crystalline phase exhibits a ring−NMe_2 substituent twist angle δ_N of 83° with an almost eclipsed ring configuration and an orientation of the nitrogen lone pair away from the ring (Figure 1). The crystal structure of the trimethylammonium tartrate salt of **(*S*)-1** exhibits a twist angle δ_N of 94° but contains a mixture of eclipsed and staggered conformers.[25] NOE experiments on **1** and related compounds[13a,26] indicate that this substituent conformation is retained in solution.

Initial adduct formation to give **1i** has been modeled through binding of a $(Me_2O)_2LiMe$ fragment to the amine nitrogen. Methyllithium was modeled as co-

valently bound, while the amine nitrogen and the two ether molecules were coordinated with distance restraints (N−Li = 2.0 Å, k_S = 500 kcal mol^{-1} Å^{-2}; O−Li = 1.85 Å, k_S = 500 kcal mol^{-1} Å^{-2}).[27,28] The geometry about the lithium was defined by setting the C_{Me}−Li−O angle at 120° with a low restraint of 20 kcal mol^{-1} deg^{-2} to mimic the coordination of the ether lone pairs. Defining lone pairs or using a more realistic C_{Me}−O−Li angle of 105° increases the complexity of exploration of conformational space due to the differentiation of ether binding orientations. Execution of all three approaches for **1i** shows that, although absolute energies change slightly, relative energies and important structural parameters for energy minima do not change. Because of the saving in computational effort, only the first approach was adopted in all other cases. Additional MM parameters used are listed in the Experimental Section.

A search of ring-substituent conformational space for the adduct **1i** identifies the global minimum **E** with a twist angle close to that of the free amine (Figure 1). That part of the rotational profile in which the CH(NMe$_2$)LiMe(Me$_2$O)$_2$ moiety is oriented toward the metal generally lies at a higher relative energy than in the amine case. Conformations **F** and **G** correspond to the two in-plane orientations for the amine nitrogen, which lead to the two possible $_pR$ and $_pS$ ortho-lithiated intermediates **1ii** and **1iii** of differing planar chirality. While the barriers to rotation are of similar height for access to **F** and **G**, data show (Table 1) that the LiCH$_3$−H$_{ring}$ distance in **F** is shorter by about 0.6 Å. To the extent that the conversion of adduct to lithiated intermediate can be regarded as highly exothermic, these calculations are consistent with the Hammond postulate, which suggests that the transition state of a highly exothermic reaction will resemble the reactant.[29]

Scheme 2

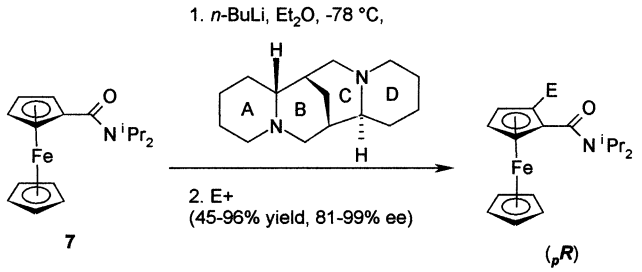

The relative energies of the lithiated intermediates **1ii** and **1iii** were also evaluated by covalent bonding of lithium to the ortho carbon using the same N−Li and Li−ether restraints.[30] In good agreement with the experimentally observed stereodifferentiation, the $_pR$,R intermediate **1ii** was favored over **1iii** by 4.4 kJ mol^{-1}, corresponding to a Boltzmann population ratio of 86:14 at 293 K, the temperature used for most syntheses. As noted previously elsewhere,[5] the greater stability of **1ii** may be attributed to minimization of the *C*-methyl interactions with the ferrocene moiety.

Conformational space above the ring is essentially free in the lithiated intermediates, and removal of the coordinated ether molecules increases the energy difference slightly to 4.6 kJ mol^{-1}. Modeling of other complexes, in which the α and N substituents were varied, was restricted to establishment of energy minima for the free amine and the ether-free lithiated intermediate. For the achiral series **8**−**11**, the CH$_2$NH$_2$ derivative **8** exhibits conformations of equivalent energy in which the NH$_2$ group is above or below the ring. Dimethyl substitution on the nitrogen or carbon forces the NR$_2$ group above or below, respectively. In the fully methylated complex **11**, the NMe$_2$ group preferentially occupies the position above the ring. In all cases, by definition, there is no energetic differentiation between the $_pR$- and $_pS$-lithiated intermediates. It is, of course, recognized that in practice the primary NH$_2$ amino group (where present) will provide the initial site for reactivity with the alkyllithium reagent. An increase in the bulk of the α substituent in the chiral CHRNMe$_2$ series switches the NMe$_2$ orientation in the global minimum energy conformation from above the ring (**1**; Me) to essentially coplanar (**12**; Ph) to below the ring (**13**; ^{i}Pr) in response to steric demand. The energy of the $_pR$,R-lithiated intermediate remains lower in all three cases, with predicted diastereoselectivities increasing in the order Me (87:13) < ^{i}Pr (96:4) < Ph (99:1). The rotational profile of the methyl ether **14** shows a global minimum which is similar to **12**, thus indicating that the principal results of this analysis may be extended to ethers.

B. Structure of Amidoferrocene Complexes. To date, the reaction given in Scheme 2 has not been widely utilized because of difficulties in functional group interconversion of the amide and the potentially limiting

(22) (a) Ledig, B.; Marsch, M.; Harms, K.; Boche, G. *Angew. Chem., Int. Ed. Engl.* **1992**, *31*, 79. (b) Boche, G.; Marsch, M.; Harbach, J.; Harms, K.; Ledig, B.; Schubert, F.; Lohrenz, J. C. W.; Ahlbrecht, H. *Chem. Ber.* **1993**, *126*, 1887. (c) Hoppe, I.; Marsch, M.; Harms, K.; Boche, G.; Hoppe, D. *Angew. Chem., Int. Ed. Engl.* **1995**, *34*, 2158. (d) Pippel, D. J.; Weisenberger, G. A.; Wilson, S. R.; Beak, P. *Angew. Chem., Int. Ed. Engl.* **1998**, *37*, 2522. (e) Ledig, B.; Marsch, M.; Harms, K.; Boche, G. *Z. Kristallogr.−New Cryst. Struct.* **1999**, *214*, 511. (f) Byrne, L. T.; Engelhardt, L. M.; Jacobsen, G. E.; Leung, W. P.; Papasergio, R. I.; Raston, C. L.; Skelton, B. W.; Twiss, P.; White, A. H. *J. Chem. Soc., Dalton Trans.* **1989**, 105. (g) Papasergio, R. I.; Skelton, B. W.; Twiss, P.; White, A. H.; Raston, C. L. *J. Chem. Soc., Dalton Trans.* **1990**, 1161. (h) Marsch, M.; Harms, K.; Zchage, O.; Hoppe, D.; Boche, G. *Angew. Chem., Int. Ed. Engl.* **1991**, *30*, 321.

(23) Wiberg, K. B.; Bailey, W. F. *Angew. Chem., Int. Ed.* **2000**, *39*, 2127.

(24) In all cases, the profiles for the opposite enantiomer are mirror images. The $_pR$ designation is used to indicate the case where the electrophile introduced after quenching has a higher Cahn−Ingold−Prelog priority than CHMe(NMe$_2$), though lithium itself has a lower priority.

(25) Luo, Y. G.; Barton, R. J.; Robertson, B. E. *Can. J. Chem.* **1987**, *65*, 2756.

(26) Butler, I. R.; Cullen, W. R.; Herring, F. G.; Jagannathan, N. R. *Can. J. Chem.* **1986**, *64*, 667.

(27) The Li−N distance of 2.0 Å was assigned on the basis of a survey of 31 crystal structures in the Cambridge Crystallographic Data Base[49] containing Li−sparteine, Li−diammine or Li−monoammine moieties in similar bonding environments. The average Li−N distance is 2.12 ± 0.05 Å (2.09 ± 0.05 Å using only the Li−sparteine structures). A slight underestimation gives good agreement in the MM calculations with k_s = 500 kcal mol^{-1} Å^{-2}.

(28) The Li−O distance of 1.85 Å was assigned on the basis of a survey of 72 crystal structures from the Cambridge Crystallographic Data Base[49] containing Li−ether or Li−carbonyl groups. The average Li−O distance was 1.95 ± 0.05 Å. A slight underestimation gives good results in the MM calculations with k_s = 500 kcal mol^{-1} Å^{-2}. A survey of the Li−carbonyl adducts gives an average Li···O=C angle of 140.5 ± 17°, thus justifying the weak restraint placed on this angle.

(29) Isaacs, N. S. *Physical Organic Chemistry*, 2nd ed.; Longman Group: Essex, U.K., 1995.

(30) The Li−C_{ring} bond stretch parameters used (Table 5) were found to give good agreement with an average Li−C_{ring} distance of 2.08 ± 0.04 Å derived from a survey of 14 nonaggregated aryllithium structures retrieved from the Cambridge Crystallographic Data Base.[49]

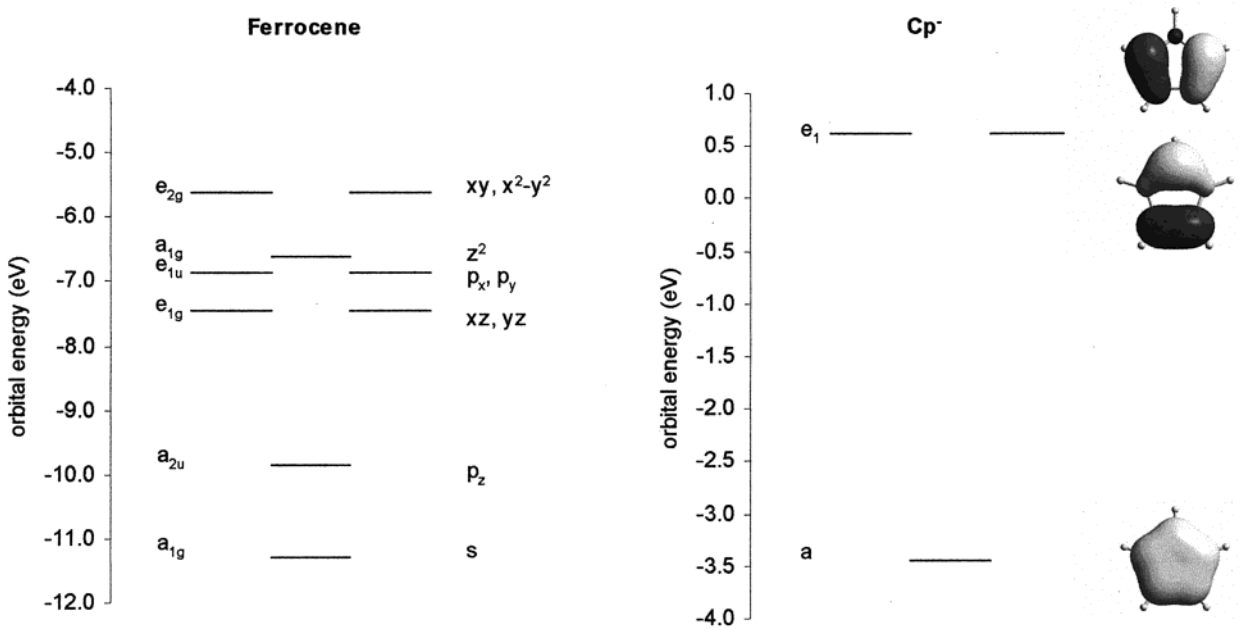

Figure 2. Molecular orbital diagrams for ferrocene and $[C_5H_5]^-$.

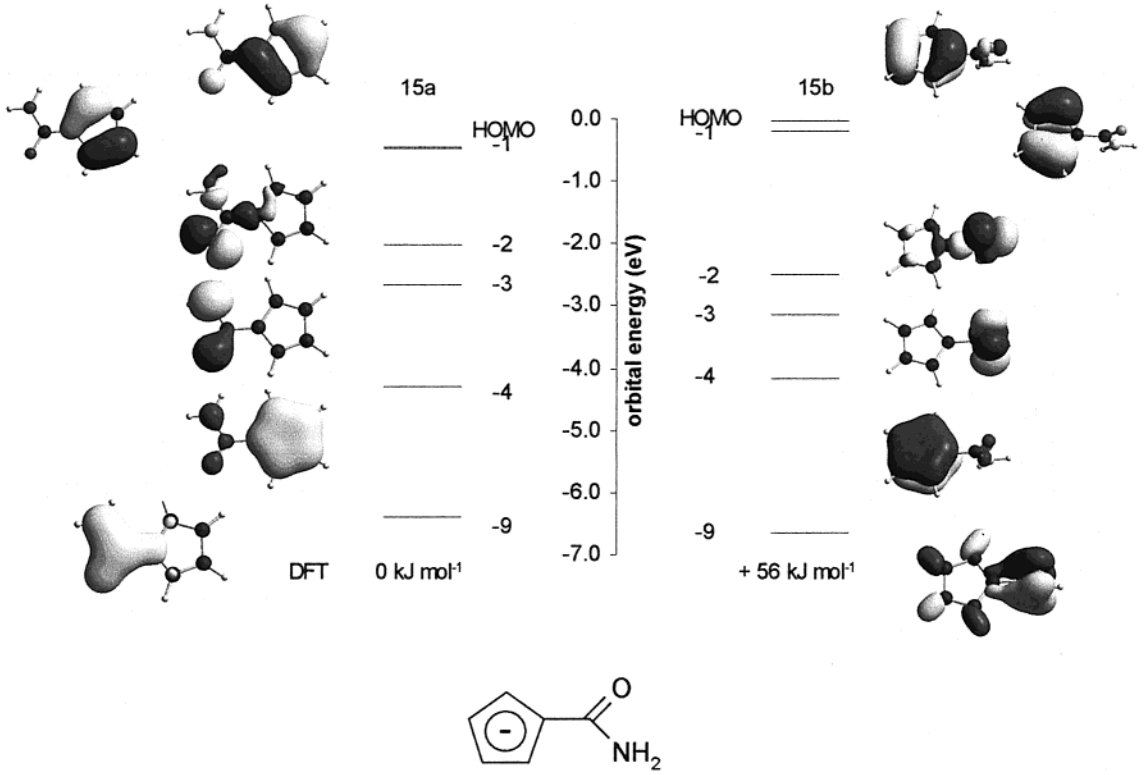

15

Figure 3. Molecular orbital diagram for $[C_5H_4C(O)NH_2]^-$.

factor of availability of only (−)-sparteine. Nevertheless, an understanding of selectivity may aid in the development of other auxiliaries or the use of a wider variety of substrates. For example, recent results on the lithiation of *N*-Boc-pyrrolidines with synthetic sparteine analogues indicate that the D ring of sparteine is superfluous.[31]

For the MM force field, the key parameter required for extension to ferrocenyl complexes containing cross-conjugated substituents such as amide is that for the torsional motion about the ring−amide bond. In the derivation and validation of this parameterization, we have used a combination of DFT calculations on the free and Fe-bound substituted-cyclopentadienyl ligands, a comparison with solid-state structural data, and indirectly, VT NMR spectroscopy.

(a) DFT Calculations. In a qualitative sense, bonding in an acceptor-substituted cyclopentadienyl complex may be represented by the resonance structures **I** and

(31) Harrison, J. R.; O'Brien, P.; Porter, D. W.; Smith, N. M. *Chem. Commun.* **2001**, 1202.

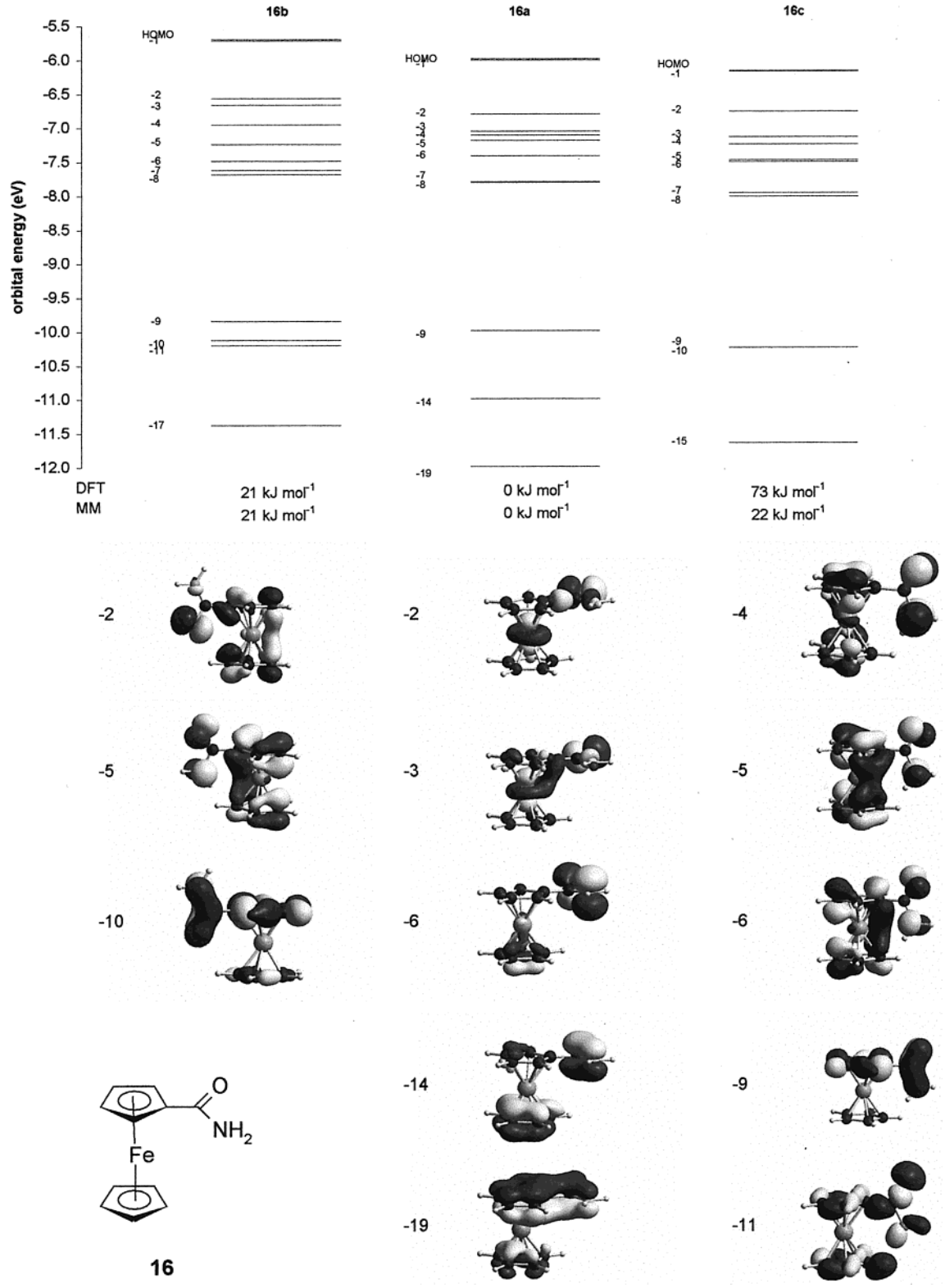

Figure 4. Molecular orbital diagram for $(C_5H_5)Fe(C_5H_4C(O)NH_2)$.

II. While **I** will be favored by hard acid counterions such

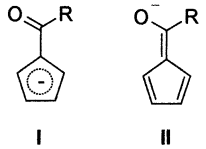

as Li^+, π-bound counterions such as Fe^{II} will favor **II**. Consistent with this picture, the ring−CHO rotational barrier for KC_5H_5CHO (61 kJ mol^{-1})[32] exceeds that of formylferrocene (37 kJ mol^{-1}).[33]

The nature of the bonding in ferrocene is well-established. The lower energy orbitals involve bonding combinations of appropriate cyclopentadienyl orbitals

(32) Arthurs, M.; Al-Daffaee, H.; Haslop, J.; Kubal, G.; Pearson, M. D.; Thatcher, P.; Curzon, E. *J. Chem. Soc., Dalton Trans.* **1987**, 2615.
(33) Sandstrom, J.; Seita, J. *J. Organomet. Chem.* **1976**, *108*, 371.

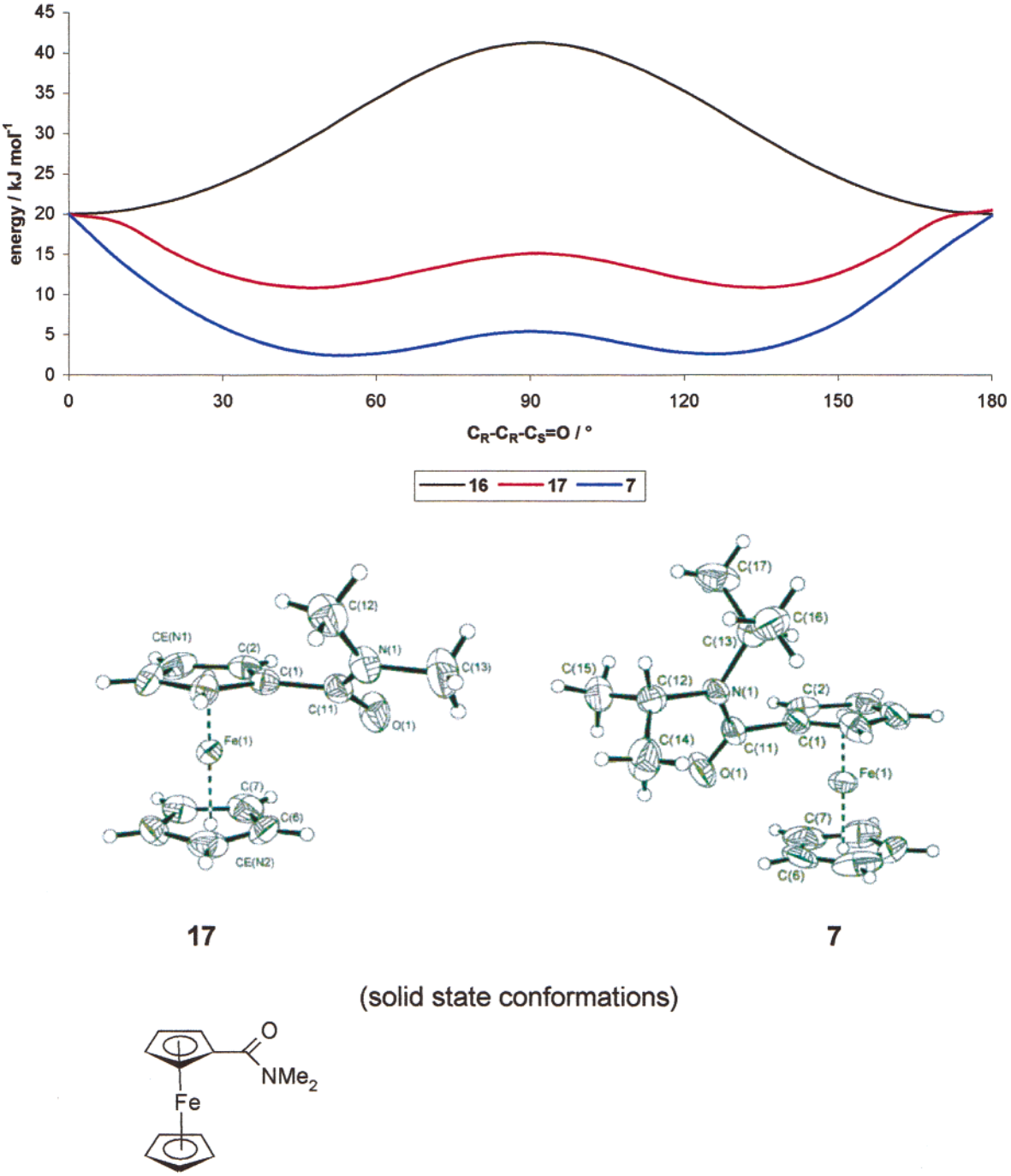

Figure 5. Substituent rotational energy profiles for $(C_5H_5)Fe(C_5H_4C(O)NR_2)$ (R = H, Me, ^{i}Pr).

with the metal d_{xz}, d_{yz}, p_z, and s orbitals. The next highest orbitals are mainly ligand-based, possibly with some contribution from the metal p_x and p_y orbitals. At highest energy are three essentially metal-based orbitals derived from $d_{xy}/d_{x^2-y^2}$ and d_{z^2}. Though photoelectron spectroscopy indicates that the HOMO is d_{z^2},[34] ab initio and DFT calculations vary in the ordering of these metal-based orbitals.[35] The calculation method adopted here (see Experimental Section) identifies the $d_{xy}/d_{x^2-y^2}$ as the HOMO for ferrocene (Figure 2), although the main conclusions derived from the calculations do not depend significantly on the ordering of these orbitals.

The MO diagram of the optimized in-plane configuration of the amidocyclopentadienyl anion **15a** (Figure 3) shows a HOMO, HOMO-1 and HOMO-4, which may be correlated with the e_1 and a orbitals of $C_5H_5^-$. The remaining orbitals comprise an oxygen lone pair (HOMO-2) of relevance to directed lithiation and nonbonding and bonding $CONH_2$ orbitals (HOMO-3 and -9). The latter contains a substantial C_1 contribution, which represents

(34) Green, J. C. *Struct. Bonding* **1981**, *43*, 37.

(35) (a) Waldfried, C.; Welipitiya, D.; Hutchings, C. W.; de Silva, H. S. V.; Gallup, G. A.; Dowben, P. A.; Pai, W. W.; Zhang, J.; Wendelken, J. F.; Boag, N. M. *J. Phys. Chem. B* **1997**, *101*, 9782. (b) Lin, L.; Berces, A.; Kraatz, H. B. *J. Organomet. Chem.* **1998**, *556*, 11. (c) Schrekenbach, G. *J. Chem. Phys.* **1999**, *110*, 11936. (d) Barlow, S.; Bunting, H. E.; Ringham, C.; Green, J. C.; Bublitz, G. U.; Boxer, S. G.; Perry, J. W.; Marder, S. R. *J. Am. Chem. Soc.* **1999**, *121*, 3715. (e) Barlow, S.; Drewitt, M. J.; Dijkstra, T.; Green, J. C.; O'Hare, D.; Whittingham, C.; Wynn, H. H.; Gates, D. P.; Manners, I.; Nelson, J. M.; Pudelski, J. K. *Organometallics* **1998**, *17*, 2113. (f) Grigorov, M. G.; Weber, J.; Vulliermet, N.; Chermette, H.; Tronchet, J. M. J. *J. Chem. Phys.* **1998**, *108*, 8790.

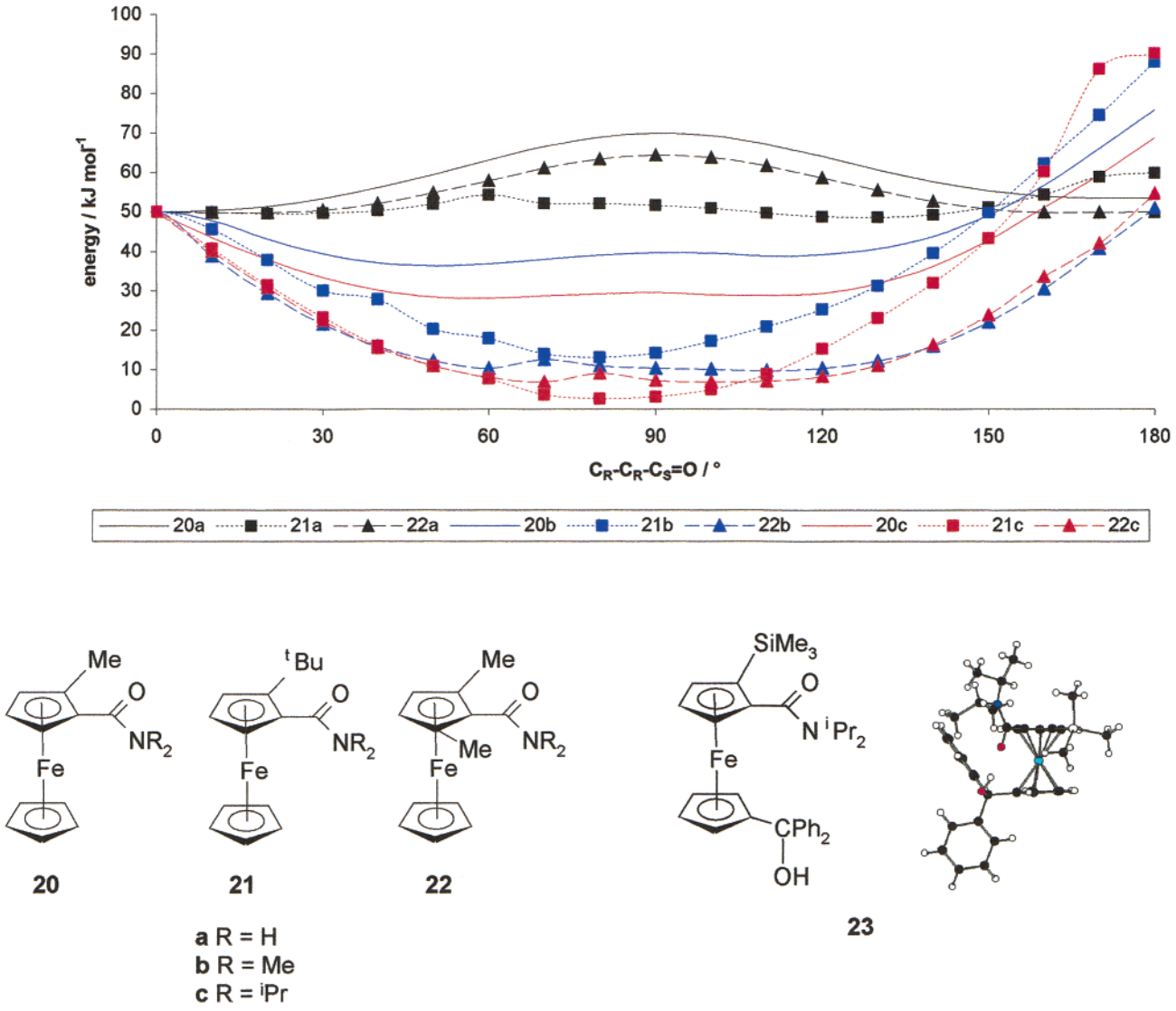

Figure 6. Molecular orbital diagram for $[C_5H_4C(NH)OH]^-$.

the main source of ring-substituent conjugation. A single-point calculation on the out-of-plane conformation **15b** shows it to be less stable by 56 kJ mol^{-1}, but with a similar configuration of molecular orbitals.

The optimized ferrocene carboxamide **16a** (Figure 4) retains the key features of ring-substituent bonding, namely a localized nonbonding $CONH_2$ orbital (HOMO-6) and a bonding $CONH_2$ orbital with stabilizing and destabilizing interactions with ring/metal orbitals (HOMO-14, -19). The HOMO, HOMO-1, HOMO-4, -5, HOMO-7, -8, and HOMO-9 orbitals may be correlated with ferrocene type e_{1u}, e_{1g}, and a_{2u} interactions. As noted elsewhere,[35b] the remaining metal-centered orbital undergoes interaction with the oxygen lone pair (HOMO-2, -3). Of the two out-of-plane conformations **16b**,**c**, the less stable is **16c**. In **16c**, the oxygen lone pair is localized, while the e_{1u} type orbitals undergo interaction with the $CONH_2$ nonbonding combination (HOMO-4 to -6). In the more stable **16b**, the oxygen lone pair undergoes interactions with one of the e_{1u} type orbitals (HOMO-2, -5). The amide bonding orbital is localized in both **16b** and **16c**.

The relative energy of the lowest energy perpendicular conformation, **16b**, was used for the parameterization of the ring−$CONH_2$ MM torsional parameter. A single-point MM calculation using the parameters listed provides a rotational barrier (22 kJ mol^{-1}) in good agreement with that calculated by DFT (21 kJ mol^{-1}). A driver calculation using these parameters provides a satisfactory MM rotational profile for the O_{down} transition state, though the value for the O_{up} transition state is less than that calculated by DFT (Figure 4). This may be attributed to a repulsive interaction between the amide σ-bond network and the eclipsed C−H bond of the unsubstituted ring (HOMO-11). Note, however, that in contrast to MM, the single-point DFT calculations do not permit ring−substituent bending, metal−ring bending or ring−ring torsion, which might be expected to relieve this interaction.

(b) Comparison with Solid-State Structures. The small magnitude of the ring−$CONH_2$ torsional barrier (21−22 kJ mol^{-1}) indicates that significant steric interactions may produce out-of-plane distortions. While an in-plane conformation is predicted for **16**, MM rotational profiles for the N^iPr_2 and NMe_2 compounds **7** and **17** anticipate ground states in which the amido group is twisted from the ring plane by 54 and 47°, respectively (Figure 5). The solid-state structures of **7** and **17**

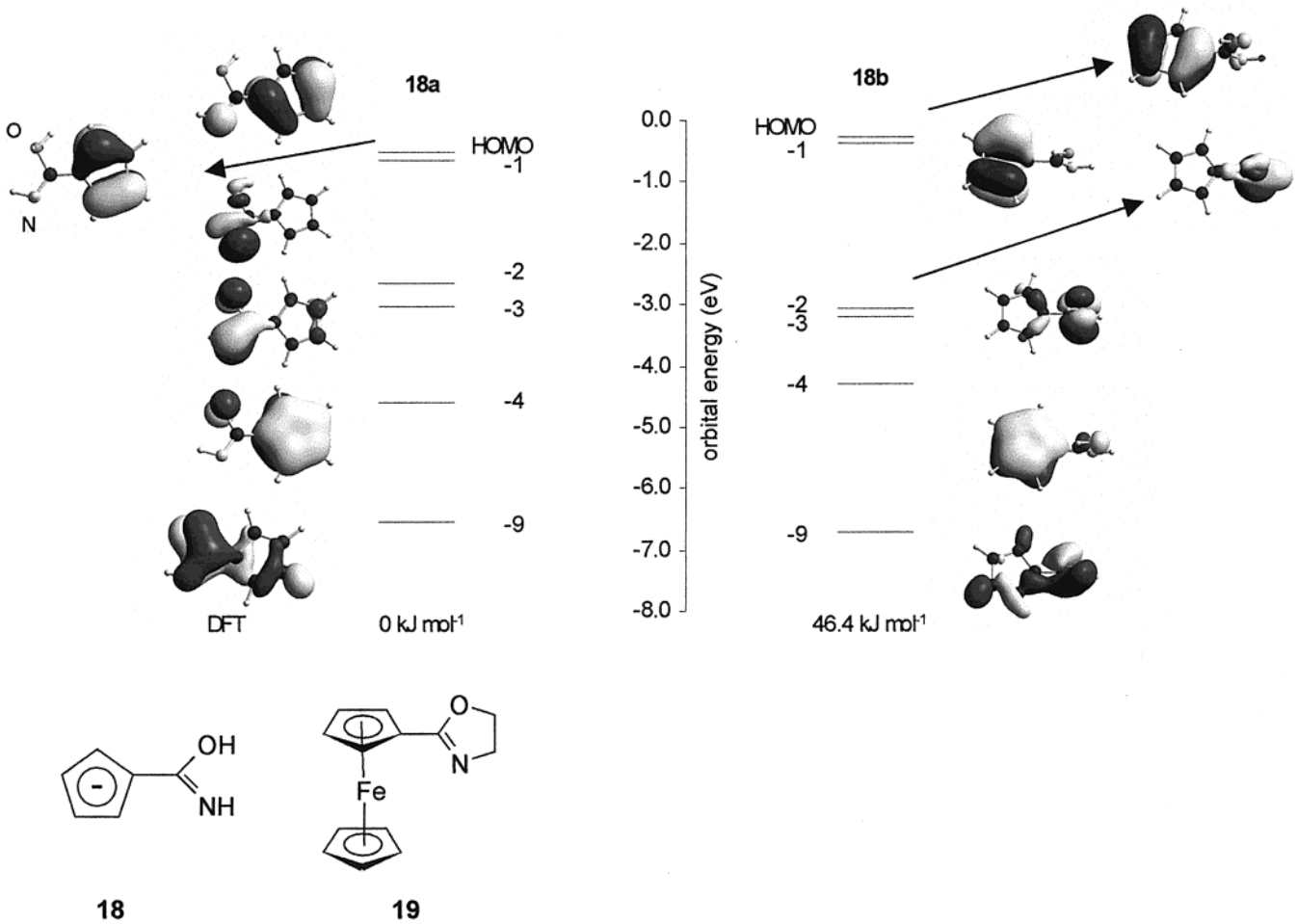

Figure 7. Substituent rotational energy profiles for *o*-substituted amide derivatives.

determined as part of this work indeed show twist angles of 64 and 37°, which are close to the predicted minima (Figure 5). The modeled ground-state structure of *N*,*N*-diisopropylbenzamide has a twist angle of 57°.[36] The effect of ortho substitution has been modeled using the 2-methyl, 2-*tert*-butyl, and 2,5-dimethyl complexes **20**−**22** (Figure 7). While the energy minima for **20** are little changed, those for **21** and **22** strongly favor nearly perpendicular orientation of the amide, with the oxygen lying below the plane of the ring. In agreement, the crystal structure of **23** exhibits a twist angle of 100°.[19a]

(c) VT NMR Spectroscopy. Consistent with the relatively low calculated torsional barriers, no selective broadening of the H_2 resonance is observed in the ^{1}H NMR for **7** or **17** down to −110 °C. On the basis of the limiting low-temperature chemical shift differences (ca. 50−100 Hz) observed for the H_2 resonance in compounds with larger barriers (for example, 37 kJ mol^{-1} in formylferrocene),[33] coalescence temperatures for ring−$CONR_2$ rotation of ca. −150 °C might be anticipated for amidoferrocenes. Both **7** and **17** do, however, exhibit typical restricted amide C−NR_2 bond rotation with barriers of 57 and 55 kJ mol^{-1}, respectively.

The place of aromatic amides in comparison to free and complexed $[C_5H_4CONH_2]^-$ should be considered. Measured barriers in tertiary 2-substituted benzamides are in the region of 60 kJ mol^{-1}, whereas tertiary 2,6-disubstituted benzamides may be isolated as atropisomers.[37] For comparison purposes, we have calculated (see Supporting Information) the energy difference between benzamide in its energy-minimized ground state and a conformation in which the $CONH_2$ group is perpendicular to the aromatic plane to be 16 kJ mol^{-1}, much closer to amidoferrocene than to the free amidocyclopentadienyl anion.

Note that the imidic acid **18** is tautomeric with the amide **15** and may be regarded as a simple free ligand model for the widely applied ferrocenyloxazoline complexes **6**. As expected, the amide tautomer **15** is more stable by 21 kJ mol^{-1}, while the *cis*-imidic acid structure shown is more stable than the trans alternative by 6.3 kJ mol^{-1}. The similarity of the MO diagrams for **15a**,**b** and **18a**,**b** (Figures 3 and 6) is obvious, and we assume that this may be extrapolated to the ferrocene complexes. The presence of a directional nitrogen lone pair in **18a** is consistent with the established directing effect of nitrogen in ortho lithiation of ferrocenyloxazoline complexes.[38] The predicted rotational barriers of **15** and **18** are comparable, and no selective broadening of the H_2 resonance is observed in the ^{1}H NMR spectra of the simple achiral oxazoline **19** down to −110 °C.

C. Lithiation of Amidoferrocenes Mediated by Sparteine. As a starting point for MM studies of the

(36) Beak, P.; Kerrick, S. T.; Gallagher, D. J. *J. Am. Chem. Soc.* **1993**, *115*, 10628.

(37) Bowles, P.; Clayden, J.; Helliwell, M.; McCarthy, C.; Tomkinson, M.; Westlund, N. *J. Chem. Soc., Perkin Trans. 1* **1997**, 2607 and references therein.

(38) Sammakia, T.; Latham, H. A. *J. Org. Chem.* **1995**, *60*, 6002.

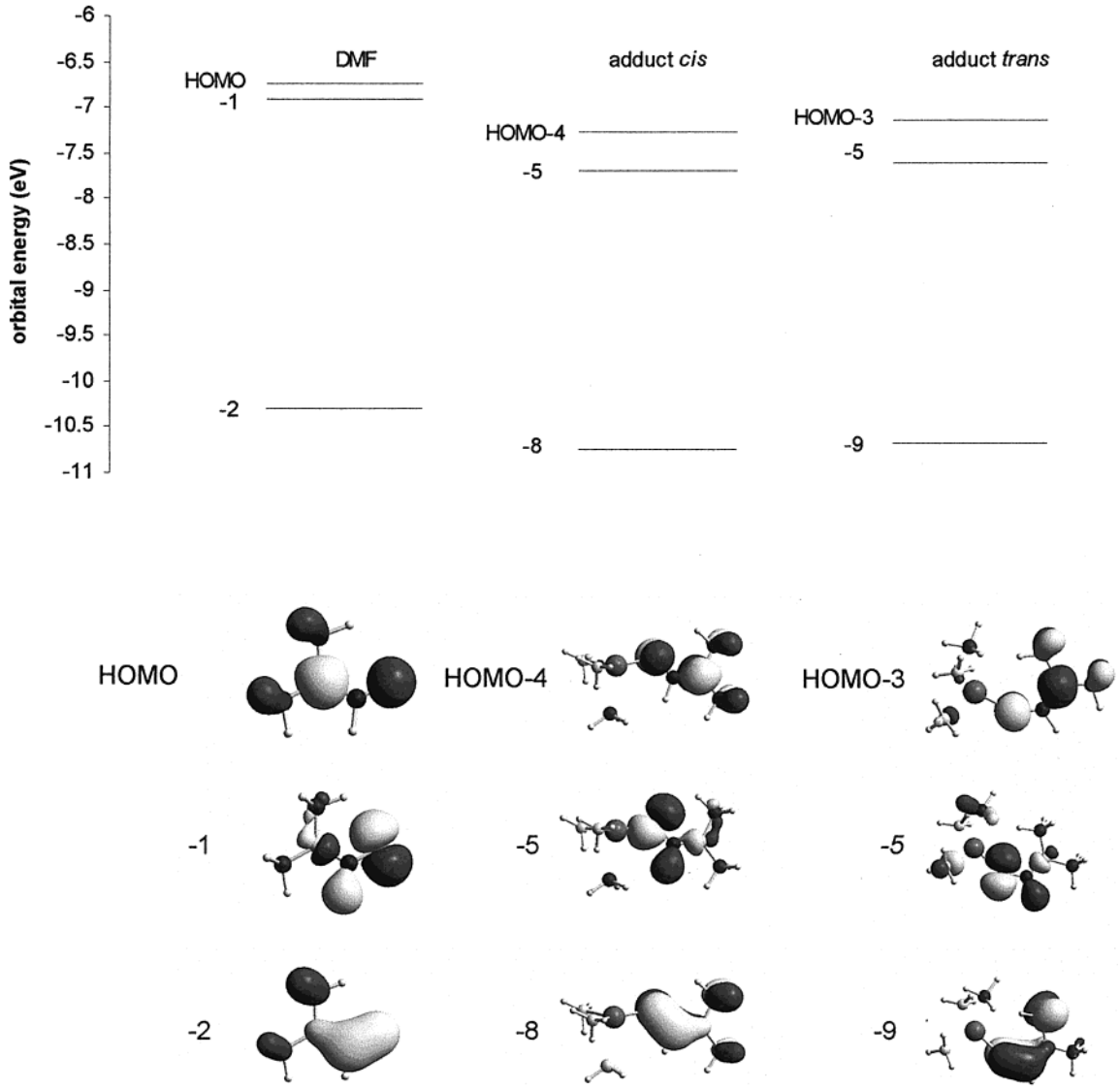

Figure 8. Molecular orbital diagrams for dimethylformamide and the $MeLi(Me_2O)_2$ adduct.

sparteine-mediated lithiation of **7**, DFT calculations have been performed on dimethylformamide and its O-bonded $MeLi(NH_3)_2$ adduct **24** to establish the geometry and conformational flexibility of $Me(NR_3)_2Li$−amide adducts (Figure 8). Calculations have been performed on both the cis and trans isomers. The cis isomer, corresponding to the geometry required for directive ortho lithiation, is more stable by 0.3 kJ mol^{-1}. The MO diagrams of **24** and dimethylformamide are similar; the lithium exhibits an orbital interaction only with the oxygen lone pair (HOMO-5). Consistent with this, the C═O stretching frequencies of alkyllithium−amide adducts are shifted only slightly to lower wavenumber relative to the free amide (1645−1655 to 1618−1625 cm^{-1}).[39] In this sterically undemanding model, there is a strong electronic preference for in-plane coordination of the lithium. Thus, a high torsional C_{ring}−C−O−Li force constant (500 kcal mol^{-1} deg^{-2}; ideal angle 0°) and a Li−O distance restraint (1.85 Å, k_S = 500 kcal mol^{-1} $Å^{-2}$) have been applied in the MM modeling of **25** and **26**, the $Me(NH_3)_2Li$ adducts of **17** and **7**, respectively. Additionally, a weak C_{amide}−O−Li angle restraint (120°, 20 kcal mol^{-1} deg^{-2}) has been applied to simulate the coordinating oxygen lone pair.[28] Anticipating sparteine coordination, the two NH_3 ligands were coordinated to the lithium via the dimensionless dummy atom **D** placed at the midpoint between the two nitrogen atoms (Li−D = 1.35 Å, D−N = 1.38 Å, 500 kcal mol^{-1} $Å^{-2}$, N−D−N = 180°, 500 kcal mol^{-1} deg^{-2}).

Sampling of conformational space for **25** and **26** through ring-substituent rotation reveals two equivalent global O_{down} minima (*pro-**R*** and *pro-**S***) at twist angles of 50 and 120° and of 50 and 140°, respectively. Local minima with C═O bent away from the iron are found at −40 and −130° and are less stable by approximately 5 and 10 kJ mol^{-1}, respectively, for the NMe_2 and N^iPr_2 derivatives. These twist angles at the energy minima are comparable to those of **7** and **17**, though the rotational barriers are much increased.

Though (−)-sparteine adopts conformation **27a** in solution and the solid state,[40] metal complexes, including organolithium derivatives,[22] contain sparteine bound in the chelating conformation **27b**.

(39) Hay, D. R.; Song, Z.; Beak, P. *J. Am. Chem. Soc.* **1988**, *110*, 8145.

(40) (a) Wiberg, K. B.; Bailey, W. F. *J. Mol. Struct.* **2000**, *556*, 239. (b) Bour, P.; McCann, J.; Weiser, H. *J. Phys. Chem. A* **1997**, *101*, 9783 and references therein.

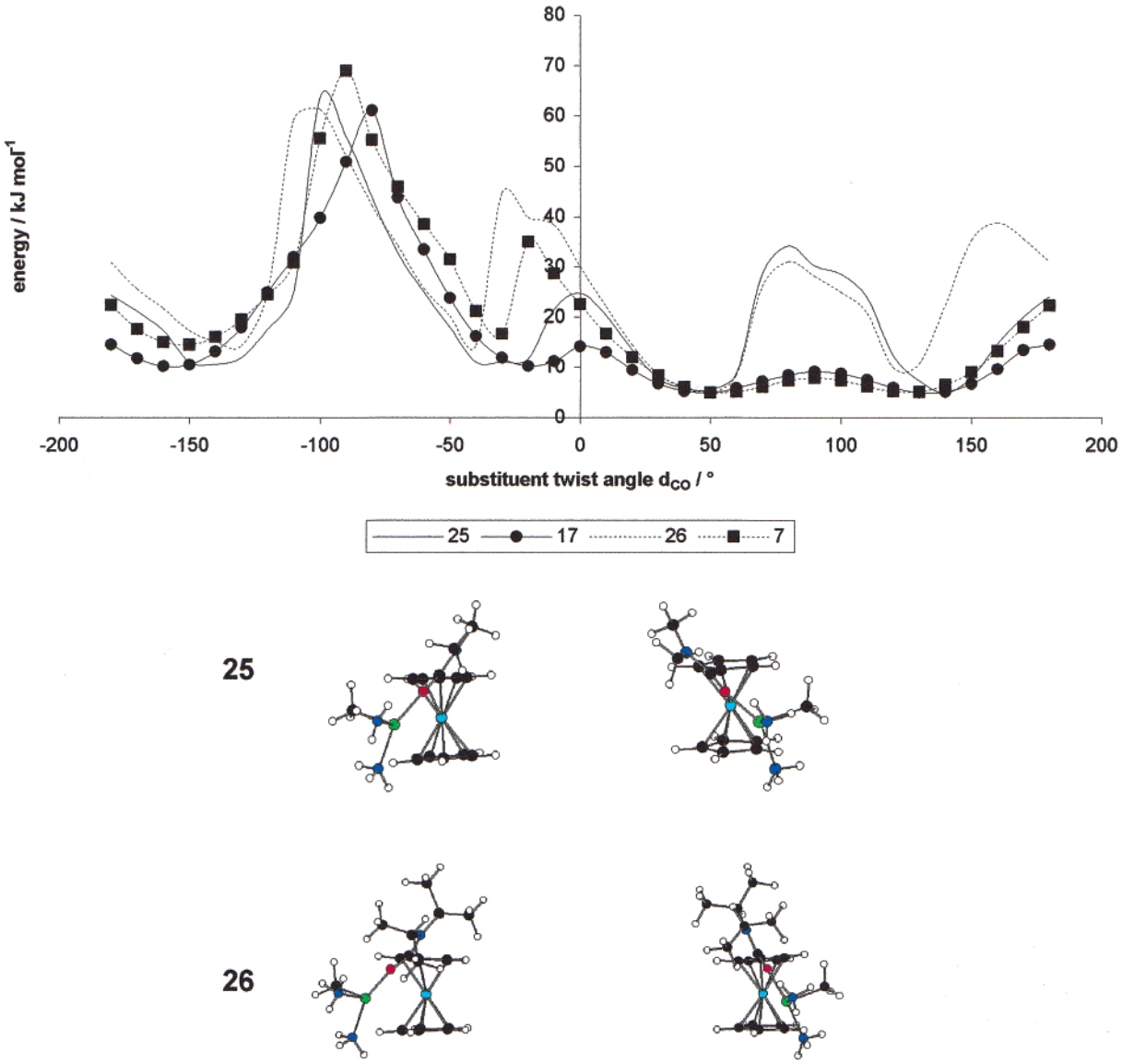

Figure 9. Substituent rotational energy profiles and structures of global minima for $Me(NH_3)_2Li$ adducts.

At the four energy minima of Figure 9, the NH_3 ligands were replaced by sparteine coordinated by a

27a **27b**

dummy atom as described (vide supra). The four energy-minimized adduct structures **28a**−**d** and **29a**−**d** obtained for the NMe_2 and N^iPr_2 derivatives are shown in Figure 10, together with appropriate structural parameters in Table 2. In response to the increased steric hindrance of the sparteine, conformations with C═O lying above the plane of the Cp ring are now more favorable. The experimentally observed selectivity is ***pS***, which seems most consistent with a selective extraction of conformer **b** from the equilibrium. Though higher in energy than conformer **a**, increased reactivity may be associated with the minimized $LiCH_3{-}H_{ring}$ interaction. As noted previously, this is consistent with the Hammond postulate, provided conversion of adduct to lithiated intermediate can be regarded as a highly exothermic process.

Inversion of chirality at the lithium itself yields diastereoisomers which lie within 10 kJ mol^{-1} of the global minima but have relevant structural parameters less favorable for subsequent ring lithiation.[41]

Energy-minimized structures of the lithiated intermediates (Figure 11) show four minima, **30a**−**d** and **31a**−**d**, which differ with respect to planar chirality and chirality at the lithium. Energy differences (Table 3) are much smaller than those of adducts **28** and **29**, and in the ***pR*** and ***pS*** diastereoisomers of lowest energy, the configuration at the lithium is opposite to that of the adduct, though by less than 2 kJ mol^{-1}. The energy barrier measured for formal diamine rotation at the lithium in (allyl)Li(tetramethylethylenediamine) adducts in diethyl ether is approximately 25 kJ mol^{-1},[42] though the exact mechanism is not established.

(41) For a similar example of stereogenic lithium in anionic cyclization, see: Bailey, W. F.; Mealy, M. J. *J. Am. Chem. Soc.* **2000**, *122*, 6787.

(42) (a) Fraenkel, G.; Cabral, J.; Lanter, C.; Wang, J. *J. Org. Chem.* **1999**, *64*, 1302. (b) See also: Fraenkel, G.; Duncan, J. H.; Martin, K.; Wang, J. *J. Am. Chem. Soc.* **1999**, *121*, 10538.

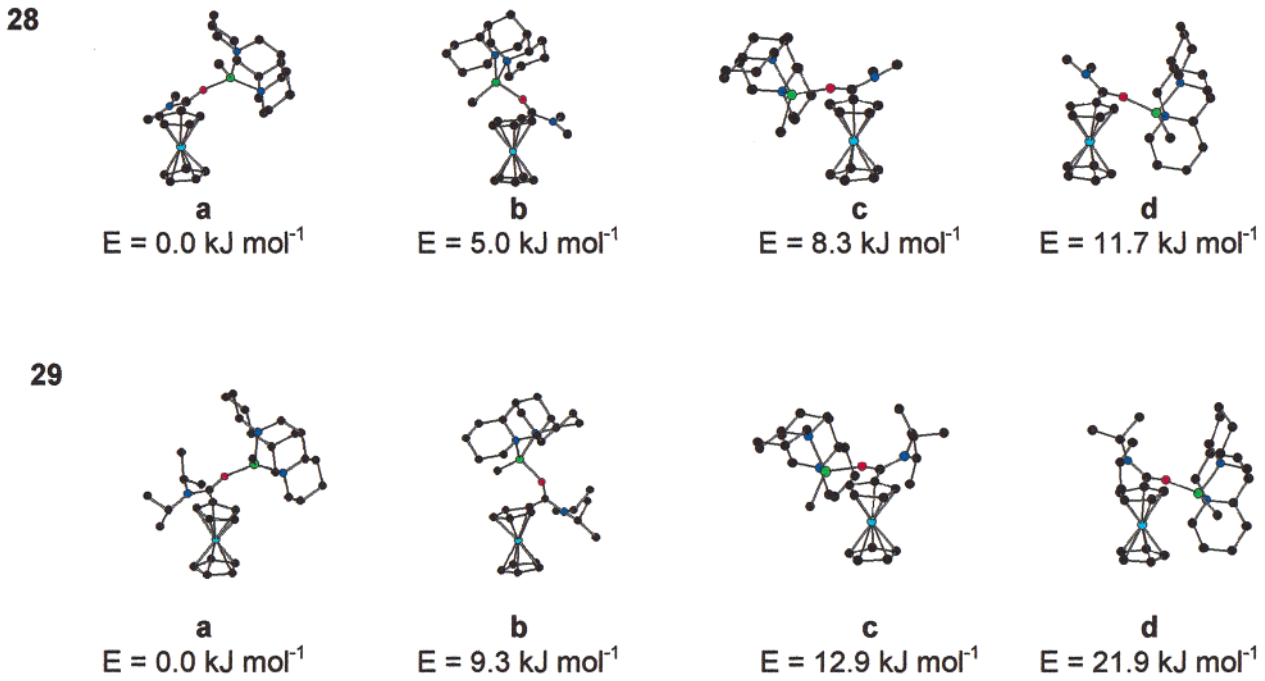

Figure 10. Energy-minimized structures of sparteine−MeLi adducts.

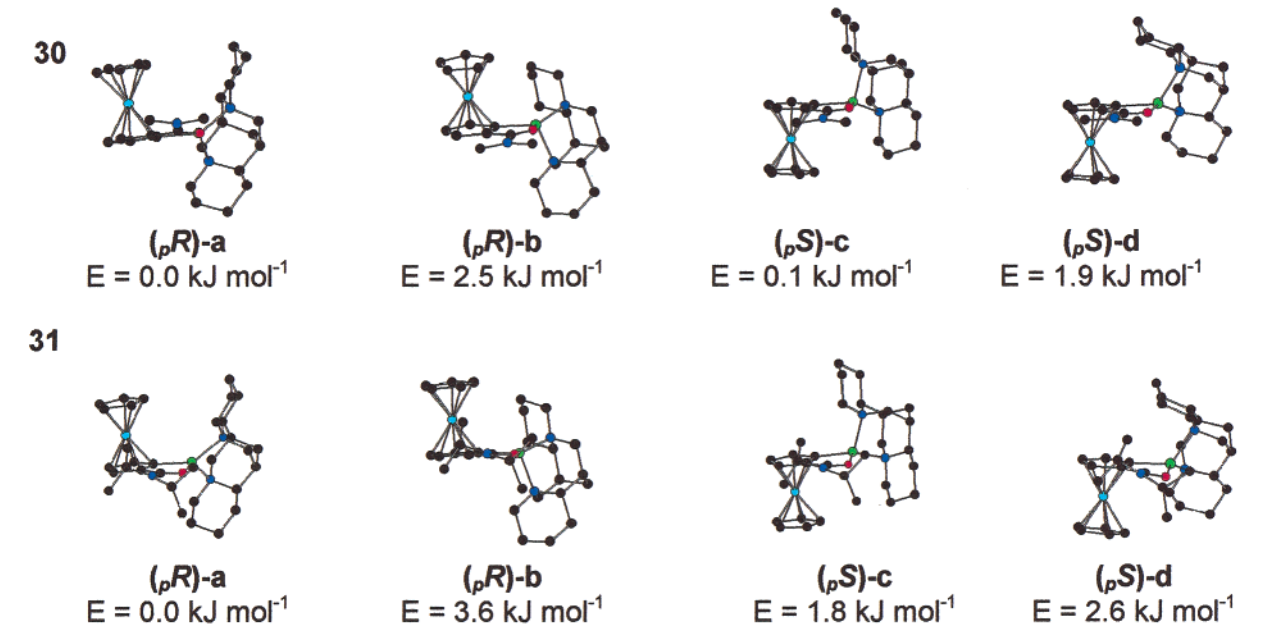

Figure 11. Energy-minimized structures of lithiated intermediates (molecules oriented down the O···Li axis with ferrocene on the left side).

Table 2. Relative Energies and Structural Parameters for Energy Minima of Sparteine−MeLi Adducts

no.	*E*/kJ mol^{-1}	pop. (195 K)/%	*pro*-$_pR$/$_pS$[a]	δ_{CO}[b]/deg	CH_3···H/Å	Li···Cfc/Å	Cfc−Cfc−H−CH_3/deg
28a	0.0	86	$_pR$	−27.6	2.90	3.33	74.2
28b	5.0	11	$_pS$	−138.4	2.72	3.36	−26.4
28c	8.3	3	$_pS$	170.5	2.91	3.49	63.8
28d	11.7	1	$_pR$	27.5	2.91	3.32	−75.0
29a	0.0	97	$_pR$	−33.4	2.92	3.24	80.2
29b	9.3	2	$_pS$	−121.9	2.76	3.43	−55.4
29c	12.9	0	$_pS$	169.3	2.91	3.55	63.5
29d	21.9	0	$_pR$	29.0	2.80	3.59	−74.8

[a] Chirality descriptors refer to lithiated intermediates. [b] $\delta_{CO} = C_{ring}-C_{ring}-C_{subst}=O$.

Table 3. Relative Conformer Energies and Populations for Energy Minima of Lithiated Intermediates

no.	$_pR$/$_pS$	*E*/kJ mol^{-1}	pop. (195 K)/%
30a	$_pR$	0.0	41
30b	$_pR$	2.5	9
30c	$_pS$	0.1	38
30d	$_pS$	1.9	13
31a	$_pR$	0.0	61
31b	$_pR$	3.6	7
31c	$_pS$	1.8	21
31d	$_pS$	2.6	12

Conclusions

Our previously published molecular mechanics force field for alkylferrocenes has been successfully extended to α-aminoferrocenes, amidoferrocenes, and other ferrocenes containing cross-conjugated substituents. The results have been applied to modeling of the diastereoselective lithiation of α-aminoferrocenes and the sparteine-mediated lithiation of amidoferrocenes. In both

Table 4. X-ray Crystallographic Data

	1	**17**	**7**
formula	$C_{14}H_{19}FeN$	$C_{13}H_{15}FeNO$	$C_{17}H_{23}FeNO$
cryst syst	orthorhombic	orthorhombic	monoclinic
a/Å	10.3214(13)	22.274(5)	6.134(2)
b/Å	13.9849(17)	17.486(5)	13.968(3)
c/Å	8.6569(11)	5.952(9)	18.692(4)
β/deg	90	90	94.7(2)
wavelength/Å	0.710 73	0.710 69	0.710 69
space group	$Pca2_1$	$Pna2_1$	$P2_1/n$
μ/mm^{-1}	1.179	1.277	0.940
Z	4	8	4
θ range/deg	1.46−28.65	2.17−25.96	2.19−21.97
no. of measd rflns	7305	2594	2251
no. of indep rflns	2892	2506	1954
R1	0.0269	0.0373	0.0794
wR2	0.0565	0.0908	0.2001

cases, it would appear that reaction proceeds via an adduct conformation which minimizes the C−H_{ring}- - - H_3C−Li distance.

Experimental Section

(a) Synthesis and NMR Spectroscopy. *rac*-**1** was obtained commercially. Compound **17** was prepared by the procedure used for **7**:[19a] mp 112−114 °C. Anal. Calcd for $C_{13}H_{15}$FeNO: C, 60.7; H, 5.84; N, 5.45. Found: C, 59.8; H, 6.00; N, 5.22. Compound **19** was prepared by a literature procedure.[43]

7. ^{1}H NMR (d_8-toluene): δ 4.48 (t, H_2), 3.89 (t, H_3), 4.22 (s, C_5H_5), 0.73, 1.49 (d, CH*Me*$_2$, J = 6.9 Hz), 2.86, 4.32 (sept, C*H*Me$_2$); T_c = 298 K, $\Delta\nu$ = 232 Hz, ΔG^*_c = 57.4 kJ mol^{-1}.

17. ^{1}H NMR (d_8-toluene): δ 4.64 (t, H_2), 4.09 (t, H_3), 4.20 (s, C_5H_5), 2.66, 2.86 (s, br, NMe$_2$); T_c = 271 K, $\Delta\nu$ = 65 Hz, ΔG^*_c = 54.9 kJ mol^{-1}.

19. ^{1}H NMR (d_2-dichloromethane): δ 4.60 (t, H_2), 4.25 (t, H_3), 4.09 (s, C_5H_5), 3.75, 4.21 (t, CH_2CH_2, J = 9.4 Hz).

^{1}H spectra were recorded on a Bruker DPX300 spectrometer; temperatures were measured using the built-in copper−constantan thermocouple previously calibrated with a platinum resistance thermometer. Rotational barriers for **7** and **17** were calculated from the equation $\Delta G^*_c = 0.01914T_c[9.972 + \log(T_c/\Delta\nu)]$.[44] On the basis of an uncertainty of ±2° in T_c, the uncertainty in ΔG^*_c is ± 0.5 kJ mol^{-1}.

(b) X-ray Crystallography. Crystals of **1** were grown by slow cooling through the melting point while being held in a 0.3 mm o.d. capillary mounted on a Stoë Stadi-4 diffractometer equipped with an Oxford Cryosystems low-temperature device. Data for **7** and **17** were collected on an Enraf-Nonius CAD4F diffractometer. Structures were solved by direct methods (SHELXS-86, SHELXS-97)[45] and refined by full-matrix least squares (SHELXL-93, SHELXL-97).[46] Data were corrected for Lorentz and polarization effects, but not for absorption. Hydrogen atoms were included in calculated positions with thermal parameters 30% larger than the atom to which they were attached. Non-hydrogen atoms were refined anisotropically. For **17**, space groups Nos. 33 and 62 were both consistent with the systematic absences, but all attempts to solve or refine the structure in space group No. 62 were unsuccessful. Crystal data for **1**, **17**, and **7** are given in Table 4.

(c) Computational Studies. DFT calculations were performed on a standard 500 MHz PC using Gaussian 98W[47] with the B3PW91 hybrid functional and the LANL2DZ basis set. As this approach tends to overestimate the Fe−C distance (2.091 Å compared to the GED value of 2.064 Å in ferrocene

Table 5. Additional Force Field Parameters

Type

	mass/g mol^{-1}	descripn
Cfc	12.000	carbon (ferrocene ring)[a]
Fe	55.847	iron (ferrocene)
LP1, LPN	0.001	dummy atoms
Li	6.941	lithium

Nonbonded

	*R** (radius)/Å	ϵ (well depth)/ kcal mol^{-1}
Fe	2.200	0.020
LP1, LPN	0.001	0.001
Li	2.380	0.011

Stretching

	force constant/ mdyn Å^{-1}	equilibrium value/Å
Fe−LP1	50.000	1.630
Cfc−Cfc	8.065	1.420
Cfc−H	4.600	1.080
Cfc−C4	4.400	1.497
Cfc−Li	1.000	2.000
C4−Li	1.000	2.000
Cfc−CO	9.600	1.460

Bending

	force constant/ mdyn Å rad^{-2}	equilibrium value/deg
LP1−Fe-LP1	0.750	180.00
Cfc−Cfc−Cfc	0.430	108.00
Cfc−Cfc−H	0.360	126.00
Cfc−Cfc−C4	0.550	126.00
Cfc−Cfc−Li	0.360	126.00
H−C4−Li	0.320	109.40
C4−C4−Li	0.360	109.40
Cfc-Cfc-CO	0.600	126.00

Out of Plane

	force constant/ mdyn Å rad^{-2}
Cfc−Li	0.050

Torsions

	V_1/kcal mol^{-1}	V_2/kcal mol^{-1}	V_3/kcal mol^{-1}
*−Cfc−Cfc−Li	0.000	15.000	0.000
Cfc−Cfc−CO−O1	1.530	2.000	0.830
Cfc−Cfc−CO−C4	−2.300	2.750	0.000
Cfc−Cfc−CO−H	0.500	2.750	0.000
Cfc−Cfc−CO−N2	0.000	0.750	0.000
Cfc−CO−N2−CO	0.000	5.000	0.000

[a] The new atom type Cfc corresponds to type Ca (aromatic carbon), with modifications to reproduce the ferrocene geometry. Only modified parameters are listed.

(43) Chesney, A.; Bryce, M. R.; Chubb, R. W. J.; Batsanov, A. S.; Howard, J. A. K. *Synthesis* **1998**, 413.

(44) Sandstrom, J. *Dynamic NMR Spectroscopy*; Academic Press: London, 1982; pp 96−97.

(45) Sheldrick, G. M. *Acta Crystallogr.* **1990**, *46A*, 467.

(46) (a) Sheldrick, G. M. SHELXL-93, A Computer Program for Crystal Structure Determination; University of Göttingen, Göttingen, Germany, 1993. (b) Sheldrick, G. M. SHELXL-97, A Computer Program for Crystal Structure Determination; University of Göttingen, Göttingen, Germany, 1997.

(47) Frisch, M. J.; Trucks, G. W.; Schlegel, H. B.; Scuseria, G. E.; Robb, M. A.; Cheeseman, J. R.; Zakrzewski, V. G.; Montgomery, J. A., Jr.; Stratmann, R. E.; Burant, J. C.; Dapprich, S.; Millam, J. M.; Daniels, A. D.; Kudin, K. N.; Strain, M. C.; Farkas, O.; Tomasi, J.; Barone, V.; Cossi, M.; Cammi, R.; Mennucci, B.; Pomelli, C.; Adamo, C.; Clifford, S.; Ochterski, J.; Petersson, G. A.; Ayala, P. Y.; Cui, Q.; Morokuma, K.; Malick, D. K.; Rabuck, A. D.; Raghavachari, K.; Foresman, J. B.; Cioslowski, J.; Ortiz, J. V.; Stefanov, B. B.; Liu, G.; Liashenko, A.; Piskorz, P.; Komaromi, I.; Gomperts, R.; Martin, R. L.; Fox, D. J.; Keith, T.; Al-Laham, M. A.; Peng, C. Y.; Nanayakkara, A.; Gonzalez, C.; Challacombe, M.; Gill, P. M. W.; Johnson, B. G.; Chen, W.; Wong, M. W.; Andres, J. L.; Head-Gordon, M.; Replogle, E. S.; Pople, J. A. *Gaussian 98*, revision A.6; Gaussian, Inc.: Pittsburgh, PA, 1998.

itself) compared to more sophisticated, but more computationally expensive, basis sets, the Fe−C distance was restricted to 2.066 Å in all calculations. HyperChem 5.11 Suite[48] was used for molecular mechanics calculations, treating the ferrocene moiety as described in ref 20. Structures were optimized using the MM+ force field (based on Allinger's MM2(91)), supplemented by the parameters listed in Table 5. Optimizations were performed in vacuo using the Polak−Ribière minimization algorithm and a root-mean-squared gradient of 0.075 kcal $Å^{-1}$ mol^{-1} as convergence criterion.

Acknowledgment. We acknowledge the use of the EPSRC Chemical Database Service at Daresbury (J.A.S.H.) and the University of Keele and the Society of Chemical Industry for the award of a Graduate Teaching Assistantship and a Messel Scholarship (N.F.).

Supporting Information Available: Tables of crystallographic data and structure refinement details. This material is available free of charge via the Internet at http://pubs.acs.org.

OM020556Q

(48) HyperChem 5.11; Hypercube Inc., Gainesville, FL 32601.
(49) Fletcher, D. A.; McMeeking, R. F.; Parkin, D. *J. Chem. Inf. Comput. Sci.* **1996**, *36*, 746.